Seismic Performance Evaluation of Inerter-based Tuned Mass Dampers dampers

A. Javidialesaadi[1], N.E. Wierschem[2]

1 Assistant Professor, Dept. of Civil and Environmental Engineering, University of Tennessee, Knoxville, United States.
E-mail: nwiersch@utk.edu
2 PhD Student, Dept. of Civil and Environmental Engineering, University of Tennessee, Knoxville, United States.
E-mail: ajavidia@vols.utk.edu

ABSTRACT
This paper investigates the performance of inerter–based (rotational inertia) tuned mass dampers (TMDs) for passive control of single degree of freedom structures (SDOF) subjected to seismic excitation. Inerter-based tuned mass dampers have been recently developed and have shown promise at providing more effective passive control potential in comparison to traditional TMDs. By utilizing the conversion of linear motion to the localized rotational motion of a flywheel, the inerter provides a high level of "mass amplification". Optimum design and performance evaluation of different types of inerter-based devices for structures subjected to harmonic or random loading has been studied previously. However, optimum design has not been investigated considering seismic excitation. In this study, two configurations of inerter-based TMDs attached to a SDOF system are optimally designed to provide the minimum response variance. In this optimization, the devices' stiffness, damping, and rotational mass are considered. Utilizing the optimal values, the performance is investigated of two device configurations at reducing the variance of a structure's response when the structure is subjected to seismic excitation. The results of this study show that utilizing the optimum inerter-based dampers can result in an improvement in the variance of the seismic response in comparison to the TMD.

Keywords: *passive control; seismic excitation; tuned mass dampers; inerter*

1. INTRODUCTION

Tuned mass dampers (TMDs) have been proposed, investigated, and implemented to mitigate the vibration of structures [1,2]. Traditional TMDs consists of a secondary mass attached to primary mass through a spring and viscous damper. It has been shown that TMDs can be effective for the reduction of the maximum displacement and the displacement RMS of a primary SDOF structure when optimum TMD stiffness and damping are selected [2–4]. Considerable studies have been done to provide optimum design procedures of TMDs considering a range of different design criteria for random and harmonic excitations [2–8].

In addition to studies focused on random and harmonic excitations, the performance evaluation and applicability of TMDs for passively controlling structures subjected seismic excitation has been studied considerably. Based on these studies, it was found that typical TMDs which have been optimized for harmonic and random excitations are generally not beneficial for the reduction of the maximum lateral displacement of tall buildings under seismic ground excitation [9,10]. In contrast with this conclusion, it was shown that heavily damped TMDs can increase the damping of the building it is connected to and reduce a structure's maximum displacement in response to the seismic excitation [11]. It has also been demonstrated that TMDs utilizing large secondary mass [12] can be effective for the reduction of the maximum displacement of a primary structure.

While it has been demonstrated that TMDs can be more effective by utilizing a high secondary to primary structure mass ratio [12], increasing the mass of the TMD is usually very expensive. The inerter [13], which converts the linear motion to the rotational motion of a flywheel, can provide large effective inertia mass using small physical mass.

Utilizing an inerter, the rotational inertia viscous damper (RIVD) has been proposed and studied for the control of a SDOF structure [14]. The RIVD consists of rotational cylinder mass, which is driven through a ball-screw mechanism and rotates in a larger cylinder containing viscous fluid. With the addition of a tuning support spring and flywheel to the RIVD, the tuned viscous mass damper (TVMD) has been proposed and studied through shake table tests of a SDOF structure equipped with a TVMD [15]. The TVMD has also shown promising performance for use in the control of MDOF structures subjected to seismic excitation [16]. The performance evaluation and design procedure for different types of inerter-based tuned mass dampers when the primary structure is subjected to random or harmonic load can be found in [17].

By replacing the viscous mass damper in TMDs with an inerter parallel to a damper and attached in series to a tuning spring, the rotational inertia double tuned mass damper (RIDTMD) has been proposed [18]. The RIDTMD has shown superior performance, in comparison to the TMD, in the reduction of the maximum amplitude of a primary SDOF structure subjected to harmonic force excitation [18]. Alternatively, by attaching an inerter between a fixed support and the secondary mass in a TMD, the tuned mass damper inerter (TMDI) has been proposed and designed optimally for the random base excitation [19]. The performance assessment of TMDIs under white noise excitation has been investigated and shows the superiority of the TMDI in comparison to TMDs. Despite these studies of the RIDTMD and TMDI, optimum design and performance evaluation considering seismic excitation has not been studied yet.

In this paper, after presenting TMDI and RIDTMD models in the first section, the optimum design procedures for the TMDI and RIDTMD, when attached to a primary SDOF structure subjected to seismic excitation, is proposed and presented in the second section. Unlike previous optimization studies, which have considered white noise excitation, the frequency content of the seismic load is taken into account in this study. In the last sections, the effectiveness of both devices and the influence of the inertial mass in the response of SDOF structures under seismic excitation is investigated.

2. INERTER-BASED TUNED MASS DAMPERS

The inerter is the crucial part of inerter-based tuned mass dampers. In the literature, the inerter is defined as a "mechanical two-terminal devices which produce an equal and opposite force proportional to the relative acceleration between the nodes (terminals)" [13]. According to this definition, the following equation represent the inerter model:

$$F = b(\ddot{u}_1 - \ddot{u}_2) \tag{2.1}$$

In this equation, F is the force acting end nodes, $\ddot{u}_1$ and $\ddot{u}_2$ are acceleration of the mechanism's end nodes, and b is the inerter mass coefficient, which known as inertance. In the rotational inertia damper context, there are two different mechanism which have been primarily considered to physically produce this model of an inerter. These mechanisms are the ball screw mechanism and the rack and pinion mechanism, which have been used in the literature to represent the inerter for different rotational inertia devices [14,15,18]. Schematics of these mechanisms are presented in Fig.2.1.

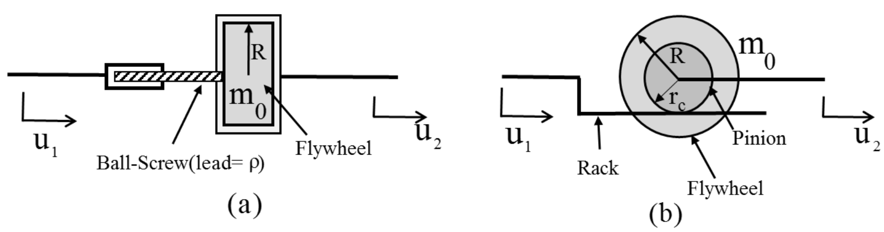

Figure 2.1: Schematic representation of mechanisms transferring translation motion of two terminals to rotation (a) Ball-Screw mechanism (b) Rack and Pinion mechanism

2.1. Tuned mass damper inerter (TMDI)

As mentioned before, the TMD consist of a secondary mass connected to primary structure through a damper and spring (Fig.2.2). With the addition of an inerter between the secondary mass and a fixed support, the tuned mass damper inerter (TMDI) (Fig.2.3) has recently been proposed and investigated when subjected to white noise base excitation [19]. In high-rise structures, one way to approximate the fixed support the inerter is attached to is to couple the inerter between the physical mass of the TMDI and an outrigger system.

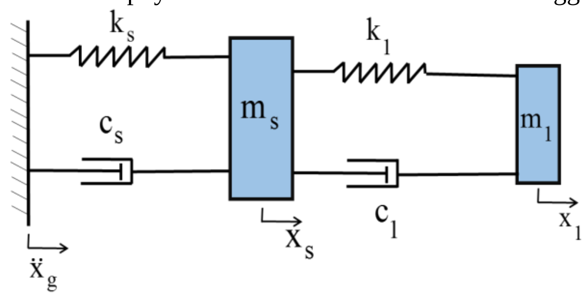

Figure 2.2 Traditional tuned mass damper (TMD)

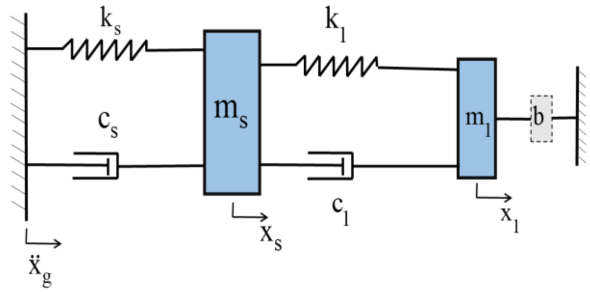

Figure 2.3 Tuned mass damper–inerter (TMDI)

The equation of motion of a SDOF structure under base excitation with a TMDI attached can be express in the following form:

$$\begin{bmatrix} m_s & 0 \\ 0 & m_1+b \end{bmatrix}\begin{Bmatrix} \ddot{x}_s \\ \ddot{x}_1 \end{Bmatrix}+\begin{bmatrix} c_1+c_s & -c_1 \\ -c_1 & c_1 \end{bmatrix}\begin{Bmatrix} \dot{x}_s \\ \dot{x}_1 \end{Bmatrix}+\begin{bmatrix} k_s+k_1 & -k_1 \\ -k_1 & k_1 \end{bmatrix}\begin{Bmatrix} x_s \\ x_1 \end{Bmatrix}=\begin{Bmatrix} m_s \\ m_1 \end{Bmatrix}\ddot{x}_g \tag{2.2}$$

where m_s is the mass of the main structure, m_1 is the secondary mass, b is the inertance (inerter equivalent mass), c_s is the main structure damping coefficient, c_1 is the secondary damping coefficient, k_s is the main structure stiffness coefficient, k_1 is the secondary system stiffness coefficient, and $\ddot{x}_g$ is the support excitation expressed in terms of acceleration. Note that the modification of the TMD in this case does not add a degree of freedom to the system.

2.2. Rotational inertial doubled tuned mass damper (RIDTMD)

The RIDTMD(Fig.2.4) is a rotational inertia damper which was developed by replacing the viscous mass damper in the TMD with an inerter parallel to a damper and attached in series to a tuning spring [18].

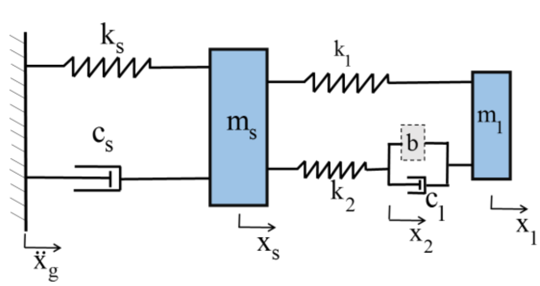

Figure 2.4 Rotational inertial double tuned mass damper (RIDTMD)

The equation of motion of a SDOF structure under base excitation with a RIDTMD attached can be express in the following matrix form:

$$\begin{bmatrix} m_s & 0 & 0 \\ 0 & m_1+b & -b \\ 0 & -b & b \end{bmatrix} \begin{Bmatrix} \ddot{x}_s \\ \ddot{x}_1 \\ \ddot{x}_2 \end{Bmatrix} + \begin{bmatrix} c_s & 0 & 0 \\ 0 & c_1 & -c_1 \\ 0 & -c_1 & c_1 \end{bmatrix} \begin{Bmatrix} \dot{x}_s \\ \dot{x}_1 \\ \dot{x}_2 \end{Bmatrix} + \begin{bmatrix} k_s+k_1+k_2 & -k_1 & -k_2 \\ -k_1 & k_1 & 0 \\ -k_2 & 0 & k_2 \end{bmatrix} \begin{Bmatrix} x_s \\ x_1 \\ x_2 \end{Bmatrix} = \begin{Bmatrix} m_s \\ m_1 \\ 0 \end{Bmatrix} \ddot{x}_g \tag{2.3}$$

where m_s is the mass of the main structure mass, m_1 is the secondary mass, b is the inertance (inerter equivalent mass), c_s is the main structure damping coefficient, c_1 is the secondary system damping coefficient, k_s is the main structure stiffness coefficient, k_1 is the secondary stiffness coefficient, k_2 is tuning stiffness coefficient, and $\ddot{x}_g$ is the support excitation. Note that the modifications to the TMD in this case adds an additional degree of freedom to the system.

3. OPTIMUM DESIGN

There are two main criteria for optimizing the TMDs and inerter-based TMDs in the literature. In the case of the harmonic load excitation, it is more common to optimize the device's parameters with the aim of minimizing the maximum displacement of the primary structure [4]. For random excitation, it is more common to obtained optimum values based on minimizing the variance of the main structure response [4,6]. In the case of seismic excitation, optimum design values considering white noise excitation can be used to minimize the RMS of the primary structure. However, in practice, seismic excitation is not like white noise and specific characteristics, such as the likely frequency content, should be taken into account. In this context, modeling of the ground motion frequency domain characteristics utilizing Kanai-Tajimi model has been done in conjunction with the determination of the optimum design values for TMD [20].

Consider $H(\omega)$ as the generic transfer function of the system in the frequency domain given a ground motion input and with the primary mass's absolute displacement as the output. The objective function for the H2 optimization problem can be write as:

$$\text{Minimize} \quad J = \frac{1}{2\pi} \int_{-\infty}^{\infty} \left| H(\omega) \right|^2 S(\omega) d\omega \tag{3.1}$$

Subject to $[k_1, c_1]$ for TMDI and $[k_1, k_2, c_1]$ for RIDTMD

In this equation, $S(\omega)$ denotes the spectral density of the ground excitation, which can be modeled with the Kanai-Tajimi spectrum as the following:

$$S(\omega) = \frac{\omega_g{}^4 + 4\xi_g{}^2 \omega_g{}^2 \omega^2}{(\omega_g{}^2 - \omega^2)^2 + 4\xi_g{}^2 \omega_g{}^2 \omega^2} \tag{3.2}$$

Where ω_g and ξ_g are the characteristic ground frequency and damping ratio, which are selected as following [20]:

ω_g =12 rad/sec and ξ_g =0.6, based on the 1940 El Centro earthquake, north-south component

ω_g =12 rad/sec and ξ_g =0.3, based on the 1995 Kobe earthquake, north-south component

The Kanai–Tajimi spectra of derived from these ground motions are shown graphically in Fig.3.1

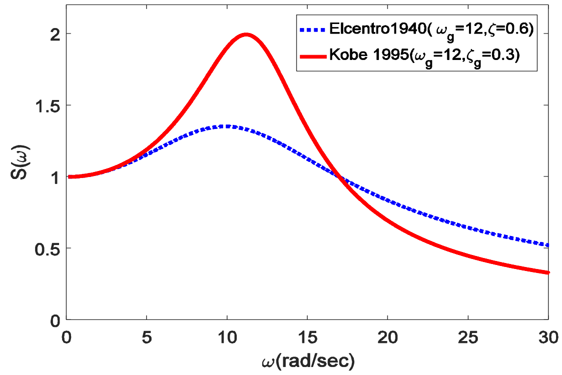

Figure 3.1 Kanai-Tajimi spectra based on ground motions

In order to consider the maximum effect of these ground motion spectra, a SDOF undamped system with the frequency equal to 12 rad/sec, the peak frequency of the ground motion spectra, is considered as the primary system. For both TMDI and RIDTMD, optimum parameters are obtained for main mass ratio ($\mu_1 = m_2/m_1$) equal to 1% and 5% via numerical optimization of Eq (3.1). For each main mass ratio, the secondary mass ratio ($\mu_2 = b/m_2$) is incrementally changed from 0.05% to 100% (step equal to 0.05%). Similarly, for the TMD, the optimum parameters were obtained for different main ratios ($\mu_1 = m_2/m_1$). In order to evaluate the performance of the optimized TMDI and RIDTMD in comparison to the optimized TMD, the following index was utilized:

$$R_{H_2} = \frac{H_{2(TMDI/RIDTMD)}}{H_{2(TMD)}} \tag{3.3}$$

In this index, H_2 represent the H2 norm of the system. The R_{H_2} index was calculated for both system when the main mass was 1% and 5% and with secondary mass ratios ranging from 0.05% to 100%.

Considering the El Centro ground motion spectrum, the effect of these mass ratios on R_{H_2} for both systems is presented in Fig.3.2. It was found for the TMDI, that the R_{H_2} decreases with increases in the secondary mass ratio (inertia mass). In other words, over the range of values considered, the performance of TMDI in the reduction of the H2 norm is always improved by increasing the secondary mass ratio. However, in the case of RIDTMD, the R_{H_2} starts decreasing with increases in the secondary mass ratio then increases with further increases in the secondary mass ratio. For example, in the case of 5% main mass ratio, a 10% secondary mass ratio provides minimum R_{H_2} and changes in the secondary mass ratio, both increases or decreases, lead to decreasing effectiveness of the RIDTMD in the reduction of the H2 norm.

Fig.3.3 shows the effect of these mass ratios on R_{H_2} from both systems considering the Kobe ground motion spectrum. The same trend is observed for both devices, R_{H_2} reduces continuously for TMDI with increases in the secondary mass. However, in the case of the RIDTMD, R_{H_2} decreases for small range of secondary mass ratios ($\mu_2 = [0.05\% - 5\%]$ for 1% , $\mu_2 = [0.05\% - 10\%]$ for 5% main mass ratio) then increases.

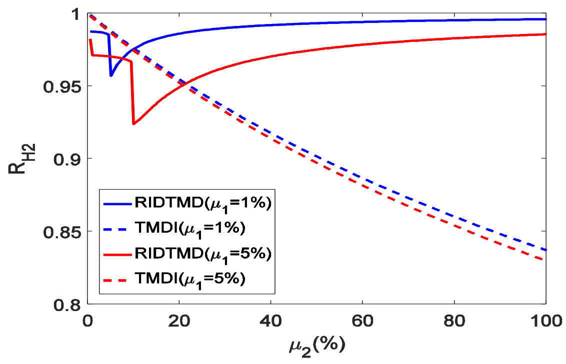

Figure 3.2 H2 Performance of RIDTMD and TMDI (El Centro Ground Motion Spectrum)

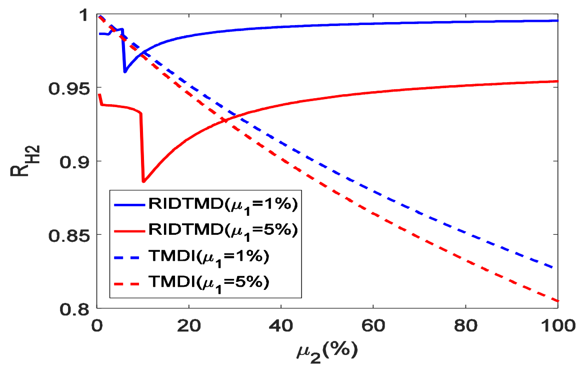

Figure 3.3 H2 Performance of RIDTMD and TMDI (Kobe Ground Motion Spectrum))

4. TIME HISTORY RESPONSE

For the time history analysis, the two earthquakes used for optimization, the 1940 El Centro earthquake, north-south component (Fig.4.1) and the 1995 Kobe earthquake, north-south component (Fig.4.2), are used to examine the performance of both dampers when the main mass ratio is equal to 1%.

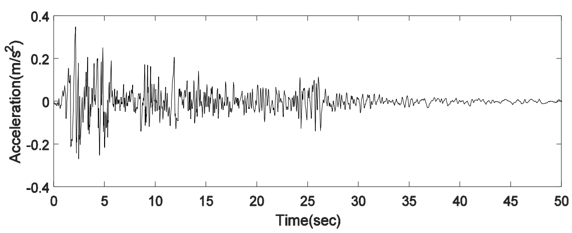

Figure 4.1 Ground acceleration (El Centro NS 1940)

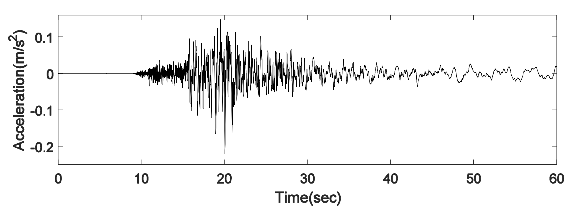

Figure 4.2 Ground acceleration (Kobe NS 1995)

In this section, a SDOF system with a TMD, TMDI, or RIDTM is considered. The optimum design values for each device are obtained from Eq. (3.1) with the Kanai–Tajimi spectra of derived from these ground motions considered as an input. Fig.4.3 show the time history response of the main structure with 100% of secondary mass ratio subjected to the El Centro ground motion. It can be found from the result that TMDI exhibits significantly superior performance, in comparison to the TMD and RIDTMD, in the reduction of the maximum displacement and the displacement RMS.

Fig.4.4 shows the time history response of the main structure with 100% of secondary mass ratio subjected to the Kobe ground motion. It can be found from the results that the TMDI once again shows superior performance in the reduction of maximum displacement and displacement RMS.

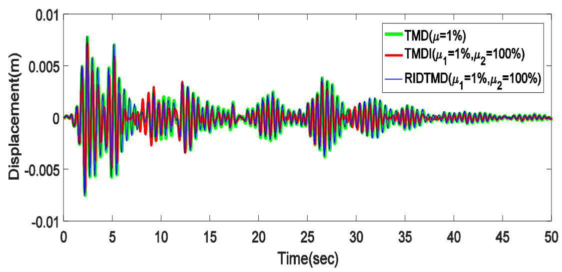

Figure 4.3 El Centro earthquake response, secondary mass ratio 100%

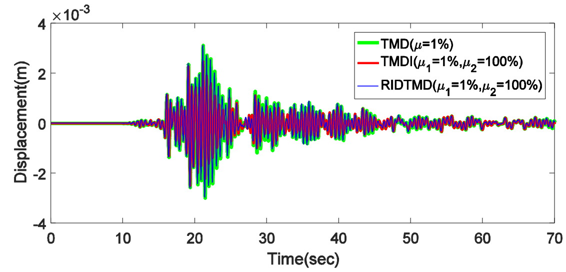

Figure 4.4 Kobe earthquake response, secondary mass ratio 100%

In contrast, when the secondary mass ratio is equal to 5%, the RIDTMD shows modest increase in performance in comparison to the TMDI and TMD (Fig.4.5 and Fig.4.6).

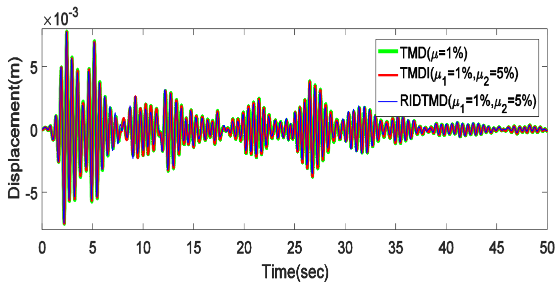

Figure 4.5 El Centro earthquake response, secondary mass ratio 5%

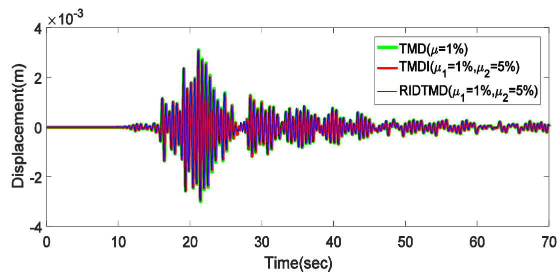

Figure 4.6 Kobe earthquake response, secondary mass ratio 5%

The quantify this, the following indices are introduced: $R_R = \frac{RMS_{RIDTMD}}{RMS_{TMD}}$ and $R_T = \frac{RMS_{TMDI}}{RMS_{TMD}}$. With these indices, the performance of TMDI and RIDTMD, in comparison to the TMD for the time history analyses shown, is presented in Table 4-1. From this table, it is found that the best TMDI performance is significantly better than RIDTMD in reduction of RMS (23%). While best performance of the RIDTMD only reduces the RMS by 5%, this is still the best performance of either the TMDI or RIDTMD when a 5% secondary mass ratio is used.

Table 4-1 Performance of TMDI and RIDTMD in reduction of RMS

	$(\mu_1 = 1\%, \mu_2 = 5\%)$ Kobe	$(\mu_1 = 1\%, \mu_2 = 100\%)$ Kobe	$(\mu_1 = 1\%, \mu_2 = 5\%)$ El-Centro	$(\mu_1 = 1\%, \mu_2 = 100\%)$ El-Centro
R_T	0.9816	0.7766	0.9792	0.7781
R_R	0.9805	0.982	0.9494	0.982

5. CONCLUSIONS

In this work, the seismic performance of two recently developed rotational inertia dampers, the tuned mass damper inerter (TMDI) and the rotational inertia double tuned mass damper (RIDTMD), are studied. H2 optimum design values of the parameters of the TMDI and RIDTMD were obtained via numerical optimization with consideration of the frequency content of the considered seismic ground motions. Utilizing the parameters obtained from the optimization, the performance of both devices was evaluated in the time and frequency domain with the results demonstrating the following points:

- Increasing the secondary mass ratio (inertial mass) of the TMDI always increases the performance in reduction of H2 norm of the main structure for the excitation spectra considered and over the range of mass ratios considered.

- Increasing the secondary mass ratio (inertia mass) of the RIDTMD does not necessarily increase the performance in reduction of H2 norm of the main structure. The performance increases and then decreases with increased secondary mass; therefore, there is an optimum secondary mass ratio for arbitrary main mass ratio that provides best performance.
- The results shows that if it is possible to use high inertial mass, the TMDI is the better option for controlling the seismic response in comparison to the RIDTMD. However, if the TMDI cannot be implemented or only a small secondary mass ratio is possible, the RIDTMD can be implemented for a modest increase in performance in comparison to the TMD.
- The time history results supports the conclusions of the frequency domain analysis.

REFERENCES

1. Frahm, H. (1909) Device for Damping Vibrations of Bodies. 989958, issued 1909.
2. Den Hartog, J. (1956) *Mechanical vibrations*, McGraw-Hill, NY.
3. Crandall, S., and Mark, W. (1973) *Random vibration in mechanical systems*, Academic Press.
4. Warburton, G.B. (1982) Optimum absorber parameters for various combinations of response and excitation parameters. *Earthq. Eng. Struct. Dyn.*, **10** (3), 381–401.
5. Wirsching, P.H., and Campbell, G.W. (1973) Minimal structural response under random excitation using the vibration absorber. *Earthq. Eng. Struct. Dyn.*, **2** (4), 303–312.
6. Asami, T., Nishihara, O., and Baz, A.M. (2002) Analytical Solutions to H[sub ∞] and H[sub 2] Optimization of Dynamic Vibration Absorbers Attached to Damped Linear Systems. *J. Vib. Acoust.*, **124** (2), 284.
7. Lee, C.-L., Chen, Y.-T., Chung, L.-L., and Wang, Y.-P. (2006) Optimal design theories and applications of tuned mass dampers. *Eng. Struct.*, **28** (1), 43–53.
8. Bakre, S.V., and Jangid, R.S. (2007) Optimum parameters of tuned mass damper for damped main system. *Struct. Control Health Monit.*, **14** (3), 448–470.
9. Sladek, J.R., and Klingner, R.E. (1983) Effect of tuned-mass dampers on seismic response. *J. Struct. Eng.*, **109** (8), 2004–2009.
10. Chowdhury, A.H., Iwuchukwu, M.D., and Garske, J.J. (1987) The past and future of seismic effectiveness of tuned mass dampers, in *Structural Control*, Springer, pp. 105–127.
11. Villaverde, R. (1985) Reduction seismic response with heavily-damped vibration absorbers. *Earthq. Eng. Struct. Dyn.*, **13** (1), 33–42.
12. Sadek, F., Mohraz, B., Taylor, A.W., and Chung, R.M. (1997) A method of estimating the parameters of tuned mass dampers for seismic applications. *Earthq. Eng. Struct. Dyn.*, **26** (6), 617–636.
13. Smith, M.C. (2002) Synthesis of mechanical networks: the inerter. *IEEE Trans. Autom. Control*, **47** (10), 1648–1662.
14. Hwang, J.-S., Kim, J., and Kim, Y.-M. (2007) Rotational inertia dampers with toggle bracing for vibration control of a building structure. *Eng. Struct.*, **29** (6), 1201–1208.
15. Ikago, K., Saito, K., and Inoue, N. (2012) Seismic control of single-degree-of-freedom structure using tuned viscous mass damper: THE TUNED VISCOUS MASS DAMPER. *Earthq. Eng. Struct. Dyn.*, **41** (3), 453–474.
16. Asai, T., Ikago, K., and Araki, Y. (2015) Outrigger tuned viscous mass damping system for high-rise buildings subject to earthquake loadings. *6AESE11ANCRiSST Jt. Conf.*
17. Hu, Y., and Chen, M.Z.Q. (2015) Performance evaluation for inerter-based dynamic vibration absorbers. *Int. J. Mech. Sci.*, **99**, 297–307.
18. Garrido, H., Curadelli, O., and Ambrosini, D. (2013) Improvement of tuned mass damper by using rotational inertia through tuned viscous mass damper. *Eng. Struct.*, **56**, 2149–2153.
19. Marian, L., and Giaralis, A. (2014) Optimal design of a novel tuned mass-damper–inerter (TMDI) passive vibration control configuration for stochastically support-excited structural systems. *Probabilistic Eng. Mech.*, **38**, 156–164.
20. Hoang, N., Fujino, Y., and Warnitchai, P. (2008) Optimal tuned mass damper for seismic applications and practical design formulas. *Eng. Struct.*, **30** (3), 707–715.